Research Article

iMedPub Journals
http://journals.imedpub.com

Journal Of Medical Physics And Applied Sciences

2017
Vol. 2 No. 1: 3

Quasi-Mono-Energetic Electron Beams from a Laser–Driven Argon Clustered Gas Target for Radiation Medicine

Mengze Tao[1], Kai Huang[2], Dazhang Li[3], Yifei Li[4], Xin Guo[4], Yong Ma[4], Jiarui Zhao[4], Minghua Li[4], Jinguang Wang[4], Nasr Hafz[5], Jie Zhang[5] and Liming Chen[6]

1 Beijing National Laboratory of Condensed Matter Physics, Institute of Physics, CAS, Beijing, China
2 Kansai Photon Science Institute (KPSI), National Institutes for Quantum and Radiological Science and Technology (QST), Japan
3I nstitute of High Energy Physics, CAS, Beijing, China
4 Beijing National Laboratory of Condensed Matter Physics, Institute of Physics, CAS, Beijing, China
5 Key Laboratory for Laser Plasmas (MOE) and Department of Physics and Astronomy, Shanghai Jiao Tong University, Shanghai, China
6 Beijing National Laboratory of Condensed Matter Physics, Institute of Physics, CAS, Beijing, China

Corresponding author: Chen L

lmchen@iphy.ac.cn

Beijing National Laboratory of Condensed Matter Physics, Institute of Physics, CAS, Beijing, China.

Tel: 861082648114

Citation: Tao M, Huang K, Li D, et al. Quasi-Mono-Energetic Electron Beams from a Laser–Driven Argon Clustered Gas Target for Radiation Medicine. Insights Med Phys. 2017, 2:1

Abstract

Purpose: To propose a promising alternative for conventional accelerators for high energy electron radiation therapy by generating quasi-mono-energetic electron beams.

Methods: Electron beams with energy up to hundred MeV, 1.8% energy spread, 125 pC charges and a few m_{rad} divergences have been achieved from a 3-mm-long clustered gas plasma, driven by laser pulse with peak power up to 100 TW. Optimization of experimental parameters, such as laser contrast and laser-plasma interaction timing leads to stable laser propagation and high-quality electron beams.

Results: Clustered gas, in addition to the self-focusing effect, owns two important features: local solid electron density and efficient absorption of ultra-short laser pulses. Therefore, high ionization levels and high electron densities could generate high-charge energetic electron beams. Our experiment has verified that clusters in the gas jet influence the laser propagation and Wakefield evolution, producing stable laser guiding and good quality electron beams.

Conclusion: The results demonstrated that the laser-driven clustered gas target provides a unique method for electron injection and has great potential in generating mono-energetic collimated electron beams with large beam charge. Stable and reproducible mono-energetic electron beams with sufficient electron intensities are required in medical applications, e.g., radiotherapy. Many engineering issues remain to be solved before clinical application, but laser-accelerated electron beams present a promising scheme for future radiation therapy.

Keywords: Laser-plasma accelerators; Clustered gas; Radiation therapy

Received: January 24, 2017; **Accepted:** February 23, 2017; **Published:** February 28, 2017

Introduction

Cluster, held together by Van-der-Walls forces, is a topic of recent interest [1-4]. When supersonic gas expands into vacuum, a multi-cluster structure is formed in a low density gas background. Compared with gas and solids, clusters appear as a novel state of matter on the nanometer scale. Owing to the great development of the chirped pulse amplification technique (CPA), the interaction of intense, ultra short laser pulses with atomic and molecular clusters [4] is an active area of research. It includes several promising applications, such as table-top plasma waveguides [5-7] relativistic particle accelerators [8-12] and X-ray sources [13,14].

Clustered gas targets, in addition to the properties of both solid

target (high local density, efficient energy absorption) and gas target (extended laser-plasma interaction length), owns their specific optical properties [15,16]. After irradiated by a high-power laser pulse, the breakdown of a cluster is initiated by optical field ionization (OFI). OFI produces the first generation of free electrons, which leads to efficient collisional ionization under local solid density. During this phase, clusters cause concave-shaped refractive index profile on the laser beam cross-section, which induces self-focusing. The use of atomic clusters presents a new scheme for efficient self-guided laser pulse propagation, in addition to relativistic self-focusing and preformed plasma waveguides.

Laser Wakefield acceleration (LWFA) [17] is foreseen as a promising scheme for the compact next generation electron accelerators. Such table-top accelerators with acceleration gradients larger than 100 GeV/m, have a great potential to replace traditional high-energy accelerators. During the last decade, experimental LWFA research has brought significant progresses in the enhancement of the electron beam quality, stability, controllability, and maximum electron energy [18-22]. For relativistic laser intensities, higher than 10^{18} W/cm^2, electrons can be completely expelled out of the focused laser volume and self-trapped in the accelerating fields associated with the plasma wave [23].

However, the self-injection regime via transverse wave-breaking is not optimal for generating quality electron beam. It requires high laser intensity a0~4 where $a_0 = eA_{laser} / mc^2$) and high plasma density (ne~10^{18} cm^{-3}), which limits the electron energy gain $E_{gain}\left(GeV\right) = 1.7\left(P/100TW\right)^{1/3}\left(n_e/10^{18}\,cm^{-3}\right)^{-2/3}$. Very recent results have shown the generation of electron beams up to 4.2 GeV from 0.3 PW laser pulses driving 9-cm-long capillary discharge waveguide at sub-10^{18} cm^{-3} density [24]. On the other hand, ionization-induced electron injection [25-28], has been realized in pure nitrogen and mixed gases to produce electron bunches with maximum acceleration length close to the dephasing length. This novel mechanism, which utilizes the large difference in ionization potentials between successive ionization states of atoms, could inject electrons into low-density laser-driven Wakefield. Nevertheless, to achieve efficient plasma channel for LWFA in a terawatt (TW) femtosecond (fs) laser, the plasma density should be above 10^{18} cm^{-3}. At this density, the electron dephasing length $L_d = \lambda_p{}^3 / \lambda_0{}^2$ (λ_p is the plasma wavelength and λ_0 is the laser wavelength) is about 1 cm and the electrons could gain a maximum energy of about 1 GeV [20] within 1-cm-long plasma channel. Efficient plasma channel guides the laser pulse to increase acceleration length up to the dephasing length Ld, above which the accelerated electrons outrun the plasma wave and slip into deceleration.

As we all know, most of the laser plasma electron accelerators have been realized with gas targets. However, clustered gas, in addition to the self-focusing effect mentioned before, owns two important features: local solid electron density and efficient absorption of ultra-short laser pulses [28]. Therefore, high ionization levels and high electron densities could generate high-charge energetic electron beams. Meanwhile, clusters also influence the Wakefield evolution and provide a source of injected electrons due to ionization by the laser field or the electron collision. It has been reported that high-charge relativistic electron beams were produced as the electrons repelled from the clusters were injected and accelerated by direct laser acceleration (DLA) [9,14,29].

For over 50 years, electron beams has been widely used in radiation therapy [30]. Conventional radiotherapy utilizes S-band linear accelerators to produce mono-energetic beams with energies of 5-20 MeV, which are used to treat skin and superficial disease [31]. However, such low-energy electrons are not qualified for deep-seated tumors. Several investigations have shown that a laser-driven electron accelerators have a great potential in direct electron and X-ray therapies [32,33]. Stable and reproducible mono-energetic electron beams with sufficient electron intensities are required in future medical applications.

In this letter, we present the generation of quasi-mono-energetic collimated (~7 mrad) electron beams generated from a clustered gas target for the first time. In our experiment, electron beams up to 210 MeV were generated by focusing a 100 TW laser pulse upon an Ar supersonic cluster-gas nozzle. Also, we demonstrated the self-focusing effect in clustered gas, causing laser-cluster interactions at high intensities.

Methods

Our schematic experimental set-up is shown in **Figure 1**.

The experiment was performed using a Ti: Sapphire laser system at the Key Laboratory of Laser Plasmas of Shanghai Jiao Tong University. Currently, the laser system delivers laser pulses of 30 fs in duration with a peak power of up to 100 TW. The laser beam was focused in vacuum by using F/20 off-axis parabolic mirror (OAP). The laser focal spot size was 30 μm in the full width at the half maximum (FWHM). Given the above laser parameters, the maximum laser intensity, and the corresponding normalized vector potential),

$$a_0 = \sqrt{\lambda^2\left(\mu m\right) I_0 \left(10^{18} W cm^{-2}\right)}$$

where 7.0 × 10^{18} W/cm-18 and 1.9, respectively. The focal point was placed above the center of a cylindrical gas jet nozzle [34] with a 3-mm diameter. The nozzle generates a supersonic Argon (99.99% purity) gas flow with a Mach number of 4.8. The gas density was controlled by varying the gas-jet stagnation pressure from 0 to 5 MPa. According to Hagena's scaling law, [1] our experiment were conducted in a slightly lower clustering level, with small cluster size and low distribution density. For example, at 3 MPa backing pressure where the quasi-mono-energetic electron beams were observed, the average cluster-gas jet density is estimated to be 3 × 10^{19} cm^{-3} [1,11,34]. The laser-plasma interaction was observed through a top-view imaging of the scattering laser light with the help of a band-pass filter. We used a 0.98 T, 16 cm long permanent dipole magnet, imaging plates (Fuji BAS-SR) and DRZ (Mitsubishi Chemical (Gd2O2S: Tb) to measure the accelerated electron beam spatial profile and

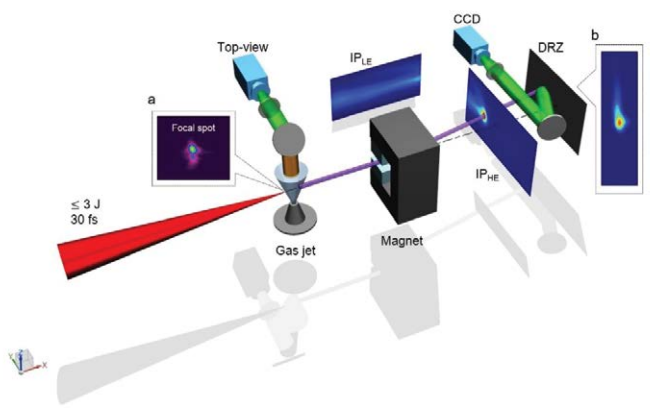

Figure 1 Schematic diagram of the experimental set-up. Inset (a) shows the optimized vacuum focal spot. The unprocessed data of electron beam energy spectrum are shown in inset (b).

energy spectrum. The magnet field disperses the electrons in the horizontal plane, which is parallel to the laser polarization. Two imaging plates wrapped by 15-μm-thick Al foil were placed right at the exits of the dipole magnet along and perpendicular to the laser propagation direction. IPHE detected undeflected betatron X-rays and energy-dispersed electrons over 100 MeV, while the low energy (LE) electrons (<100 MeV) were recorded on IPLE. Electrons below 50 MeV were deflected and hit the beam dump. The electron beam energy spectrum on the DRZ was measured using an intensified charge-coupled-device (ICCD) camera.

In experiment, we adjusted the experimental parameters, such as gas background pressure and time delay between the laser pulse and gas jet nozzle, to optimize electron beam quality. As clusters are formed by condensation of atoms in vacuum, when heated by laser pre-pulse, they would eventually expand and merge to form locally uniform plasma in 10-100 ps [5]. Therefore, the gas jet nozzle must be triggered at the right time before interaction; otherwise clusters would be unformed or destroyed at arrival of laser pulse, leading to accordingly poor plasma channels and no effective signals of electron beams. This experimental phenomenon suggests that most of the injected electrons originate from clusters. Our records show that the best guiding results, as illustrated in **Figure 2**, were achieved when the gas jet nozzle were triggered 7.8 ms before arrival of laser pulse at the background pressure of 3 MPa.

Figure 2a shows a 3-mm-long laser plasma channel achieved through the self-guiding of the laser pulse, which were observed in almost all the shots along with collimated electron beams. We also observed the laser pulse's periodically focusing and defocusing during the propagation. **Figure 2b** shows the spatial profile of a collimated electron beam observed under the optimal parameters. The horizontal and vertical divergences are 6.4 m_{rad} and 9.1 m_{rad} (FWHM), respectively.

Normally in LWFA, if the laser power exceeds the critical power for relativistic self-focusing (here $\omega 0$ is the laser frequency and ωp is the plasma frequency), a long interaction channel or filamentary channels extending to several Rayleigh lengths is expected [20]. For comparison, no effective plasma channel (< 0.5 mm) or electron beam was observed with pure helium target at the same parameters, meaning no self-guided laser propagation and self-injection occurred. The results support the fact that clusters induce intense laser pulse self-focusing and provide a novel scheme for electron acceleration.

Results

Figure 3 presents electron energy spectra obtained from imaging plates for 3 shots, which were achieved at different laser energy. Three columns present (from left to right) electron energy spectra (<100 MeV) recorded on IPLE, electron energy spectra (>100 MeV) recorded on IPHE and corresponding original energy spectra around high energy peak. Relevant information for these shots is given in **Table 1**. The corresponding laser contrast is

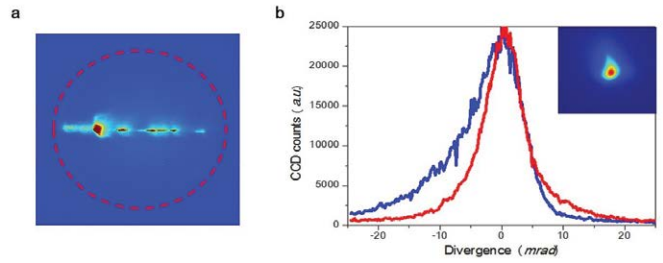

Figure 2 Plasma channel and e-beam spatial profile. (a) Top-view image of a laser-plasma channel. The red dashed line shows the outline of the gas jet nozzle. (b) The transverse spatial profile of a collimated electron beam generated from the clustered gas target (without the permanent dipole magnet). The red (blue) curve is the horizontal (vertical) lineout.

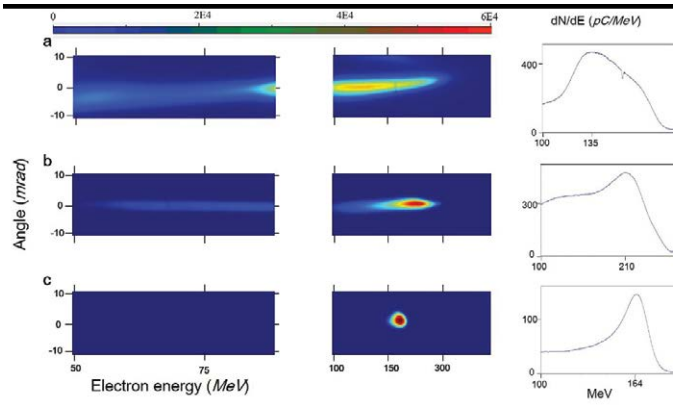

Figure 3 Energy spectra of typical quasi-mono-energetic electron beams for 3 shots at the same background pressure. The horizontal axis is the dispersive direction so that the abscissa gives information about the e-beam energy. The nondispersive direction represents the divergence of the beam. First column: electron energy spectra (< 100 MeV) recorded on IPLE; Second column: electron energy spectra (> 100 MeV) recorded on IPHE. Third column: corresponding integrated energy spectra around high-energy peak. Laser contrast increases successively (10^{-6}, 10^{-7} and 10^{-8}) from Figures 3a to 3c.

increasing successively from 10^{-6} to 10^{-8}. By using high contrast laser, the damage of clusters can be avoided. **Figure 3a** shows a typical broad energy spectrum, with peak energy ~135 MeV and total charge ~450 pC. The poor-quality beam energy spread is commonly achieved by using low laser contrast. And the beam quality increases as the laser contrast. **Figure 3b** shows the improvement in beam quality, yielding a quasi-mono-energetic e-beam of energy peak ~210 MeV, energy spread ~32% and total charge ~315 pC. Meanwhile, the high-energy front indicates electrons with energies over 300 MeV. Further optimizing laser contrast will improve a lot of the beam quality. **Figure 3c** shows a quasi- mono-energetic electron beam with energy spread ~1.8%, 164 MeV electron energy peak, and total charge ~125 pC. The calculated energy spread in **Table 1** is absolute energy spread after unfolding the contribution to the peak width due to the horizontal divergence of the electrons in the energy dispersion plane, assumed equal to the vertical divergence of the e-beam.

Our experimental results could be explained by a combination of the ionization induced injection and beam loading [35]. There is a large ionization potential difference between L-shell electrons (425 eV and 481 eV for Ar9+ and Ar10+, respectively, requiring IL ~10^{18} W/cm^{-2} to ionize) and M-shell electrons (144 eV for Ar8+, requiring IL ~4×10^{16} W/cm^{-2} to ionize). Therefore, the M-shell electrons of Ar gas are pre-ionized by the leading front of the laser pulse and form the electron sheath of the Wakefield bubble, while the inner shell electrons are collisionally ionized out of Ar clusters by the peak of the laser pulse, as well as optical-field-ionization of the gas atom. Cluster electrons oscillate back and forth by the combined effects of the laser field and the electrostatic field produced by the laser-driven charge separation [8,13]. Due to the efficient absorption of the laser pulse, the energetic electrons finally escape from the clusters [28] with enough initial energy to move at the phase velocity of the wake, they will be easily trapped and accelerated by the longitudinal electric field.

As more and more electrons are ionized out of clusters and injected into the Wakefield, which depletes the longitudinal accelerating field, the injection finally ceases because electrons do not gain enough energy to be trapped in the Wakefield. This phenomenon, known as beam loading [36], limits the total charge of the electron bunch, and results in low energy spread in our experiment. For plasma wakes in the blowout regime, significant beam loading will occur when the loaded charge Q (nC) $>$ (where is the electric field caused by the injected electrons, kp-1 is the plasma skin depth, and Rb is the blowout radius of the wake) [35].

Table 1 Laser parameters and characteristics of e-beams shown in Figure 3. E_{peak} is the energy peak in the energy spectra. Third column is the absolute energy spread after unfolding. Fourth column gives the vertical divergence of the electron beams. Total charge (over 50 MeV) is given in the fifth column. Laser contrast increases successively from a to c.

Shot	E_{peak} (MeV)	% Energy spread	Divergence (mrad)	Charge (pC)	E_{laser} (J)
a	135	51	9.3	450	2.3
b	210	32	7.4	315	3.0
c	164	1.8	6.9	125	2.6

The total loaded charge can be estimated by, considering the matched condition [37]. However, the formula didn't hold well for our case, since the laser-plasma parameters and are unmatched. When the laser contrast is high, the clusters don't suffer from the pre-pulse and guarantee direct interaction between main laser pulse and clusters. The laser-cluster interaction occurs at near solid density, providing a source of tremendous injected electrons. So, under the radiation of intense laser pulse, a large amount of electrons will be ionized out of the clusters and injected into the Wakefield [8,13]. Compared with a laser driven nitrogen gas target (typical ionization-induced electron injection regime), the injection process in this case happens much faster because of the high ionization levels and high electron densities. Hence the electron beam loads the wake immediately, i.e., the injected electrons cancel out the longitudinal accelerating field and end the injection.

Therefore, the extremely fast injection process limited by beam loading effect should be responsible for the quasi-mono-energetic electron beam in **Figure 3c** with an energy spread of only 1.8%. Meanwhile, as we decrease the laser contrast, the laser pulse guiding becomes less efficient, leading to poor plasma channels as observed. Clusters were pre-ionized by the pre-pulse before arrival of main laser pulse and increased the surrounding plasma density. It's been proven that the total loaded charge Q is proportional to plasma density np [37,38]. Accordingly, the injection process is extended relatively, thus generating e-beams of high charge and large energy spread as shown in **Figures 3a** and **3b.** Note that in **Figure 3a**, the total charge (over 50 MeV) is up to 450 pC in spite of the broad energy spectra.

Conclusion

In conclusion, the experiments have demonstrated that quasi-mono-energetic electron beams with 1.8% energy spread, peak energy ~164 MeV and high beam charge (> 50 MeV) ~125 pC can be realized using Argon clustered gas jet driven by 100 TW lasers. Optimization of experimental parameters, such as laser contrast and gas jet nozzle timing leads to stable laser propagation and high-quality electron beams. We found that clusters in the gas jet influence the laser propagation and Wakefield evolution, producing stable laser guiding and good quality electron beams. Our results indicate that the laser-driven clustered gas target provides a unique method for electron injection and has great potential in generating mono-energetic electron beams with high beam charge. Mono-energetic e-beams with stable and reproducible properties with sufficient electron intensities are achieved, which presents a promising scheme for future radiation therapy.

Acknowledgment

This work was supported by the National Basic Research Program of China (2013CBA01501), National Key Scientific Instrument and Equipment Development Project (2012YQ120047), National Natural Science Foundation of China (11334013, 11121504) and NSAF (U1530150), and the CAS key program (KGZD-EW-T05).

References

1 Hagena OF, Obert W (1972) Cluster formation in expanding supersonic jets: Effect of pressure, temperature, nozzle size, and test gas. J Chem Phys 56: 1793.

2 Boldarev AS, Gasilov VA, Ya-Faenov A, Fukuda Y, Yamakawa K (2006) Gas-cluster targets for femtosecond laser interaction: Modeling and optimization. Rev Sci Instrum 77: 083112.

3 Gao X, Wang X, Shim B, Arefiev AV, Korzekwa R, et al. (2012) Characterization of cluster/monomer ratio in pulsed supersonic gas jets. Appl Phys Lett 100: 064101.

4 Fennel TH, Meiwes-Broer KH, Tiggesbäumker J, Reinhard PG, Dinh PM, et al. (2010) Laser-driven nonlinear cluster dynamics. Rev Mod Phys 82: 1793.

5 Milchberg HM, Kim KY, Kumarappan V, Layer BD, Sheng H (2006) Clustered gases as a medium for efficient plasma waveguide generation. Phil Trans R Soc A 364: 647.

6 Kumarappan V, Kim KY, Milchberg HM (2005) Guiding of intense laser pulses in plasma waveguides produced from efficient, femtosecond end-pumped heating of clustered gases. Phys Rev Lett 94: 205004.

7 Chen LM, Kotaki H, Nakajima K, Koga J, Bulanov SV, et al. (2007) Self-guiding of 100TW femtosecond laser pulses in centimeter-scale under-dense plasma. Phys Plasmas 14: 040703.

8 Chen LM, Park JJ, Hong KH, Kim JL, Zhang J, et al. (2002) Emission of a hot electron jet from intense femtosecond-laser–cluster interactions. Phys Rev E 66: 025401.

9 Fukuda Y, Akahane Y, Aoyama M, Hayashi Y, Homma T, et al. (2007) Physics of fully-loaded laser-plasma accelerators. Phys Rev A 363:130.

10 Fukuda Y, Ya Faenov A, Tampo M, Pikuz TA, Nakamura T, et al. (2009) Energy increase in multi-MeV ion acceleration in the interaction of a short pulse laser with a cluster-gas target. Phys Rev Lett 103: 165002.

11 Zhang L, Chen LM, Wang WM, Yan WC, Yuan DW, et al. (2012) Electron acceleration via high contrast laser interacting with submicron clusters. Appl Phys Lett 100: 014104.

12 Koester P, Bussolino GC, Cristoforetti G, Faenov A, Giulietti A, et al. (2015) High-charge divergent electron beam generation from high-intensity laser interaction with a gas-cluster target. Laser Part Beams 33: 331.

13 Chen LM, Liu F, Wang WM, Kando M, Mao JY, et al. (2010) Intense high-contrast femtosecond K-shell X-ray source from laser-driven Ar clusters. Phys Rev Lett 104: 215004.

14 Chen LM, Yan WC, Li DZ, Hu ZD, Zhang L, et al. (2013) Bright betatron X-ray radiation from a laser-driven-clustering gas target. Sci Rep 3: 1912.

15 Tajima T, Kishimoto Y, Downer MC (1999) Optical properties of cluster plasma. Phys Plasmas 6: 3759.

16 Alexeev I, Antonsen TM, Kim KY, Milchberg HM (2003) Self-focusing of intense laser pulses in a clustered Gas. Phys Rev Lett 90: 10.

17 Tajima T, Dawson JM (1979) Laser electron accelerator. Phys Rev Lett 43: 267.

18 Geddes CGR, Toth CS, Van Tilborg J, Esarey E, Schroeder CB, et al. (2004) Simulation of monoenergetic electron generation via laser wakefield. Nature (London) 431: 538.

19 Leemans WP, Nagler B, Gonsalves AJ, Toth C, Nakamura K, et al. (2006) GeV electron beams from a centimetre-scale accelerator. Nat Phys 2: 696.

20 Esarey E, Schroeder CB, Leemans WP (2009) Physics of laser-driven plasma-based electron accelerators. Rev Mod Phys 81: 1229.

21 Yan WC, Chen LM, Li DZ, Zhang L, Hafz NAM, et al. (2014) Concurrence of monoenergetic electron beams and bright X-rays from an evolving laser-plasma bubble. Proc Natl Acad Sci USA 111: 5825.

22 Wang X, Zgadzaj R, Fael N, Li Z, Yi SA, et al. Quasi-monoenergetic laser-plasma acceleration of electrons to 2 GeV. Nat. Commun. 4,1988.

23 Pukhov A, Gordienko S (2006) Bubble regime of wake field acceleration: similarity theory and optimal scalings. Phil Trans R Soc A 364: 623.

24 Leemans WP, Gonsalves AJ, Mao HS, Nakamura K, Benedetti C, et al. (2014) Multi-GeV electron beams from capillary-discharge-guided sub-peta-watt laser pulses in the self-trapping regime. Phys Rev Lett 113: 245002.

25 Clayton CE, Ralph JE, Albert F, Fonseca RA, Glenzer SH, et al. (2010) Self-guided laser wakefield acceleration beyond 1 GeV using ionization-induced injection. Phys Rev Lett 105: 105003.

26 Pak A, Marsh KA, Martins SF, Lu W, Mori WB, et al. (2010) Injection and trapping of tunnel-ionized electrons into laser-produced wakes. Phys Rev Lett 104: 025003.

27 Huang K, Li DZ, Yan WC, Li MH, Tao MZ, et al. (2014) Simultaneous generation of quasi-monoenergetic electron and betatron X-rays from nitrogen gas via ionization injection. Appl Phys Lett 105: 204101.

28 Taguchi T, Antonsen TM, Milchberg HM (2004) Resonant heating of a cluster plasma by intense laser light. Phys Rev Lett 92: 205003.

29 Pukhov A, Sheng ZM, Meyer-Ter-Vehn J (1999) Particle acceleration in relativistic laser channels. Phys Plasmas 6: 2847.

30 Kainz KK, Hogstrom KR, Antolak JA, Almond PR, Bloch CD, et al. (2004) Dose properties of a laser accelerated electron beam and prospects for clinical application. Med Phys 31: 2053-2067.

31 Chiu C, Fomytskyi M, Grigsby F, Raischel F, Downer MC, et al. (2004) Laser electron accelerators for radiation medicine: A feasibility study. Med Phys 31: 2042-2052.

32 Lundh O, Rechatin C, Faure J, Ben-Ismail A, De Wagter C, et al. (2012) Comparison of measured with calculated dose distribution from a 120-MeV electron beam from a laser-plasma accelerator. Med Phys 39: 3501-3508.

33 Rassuchine J, Dyer G, Cho B, Sentoku Y, Cowan T, et al. (2006) WE-E-330D-01: The production of ultrafast bright K-alpha x-rays from laser produced plasmas for medical imaging. Med Phys 33: 2251.

34 Semushin S, Malka V (2001) High density gas jet nozzle design for laser target production. Rev Sci Instrum 72: 7.

35 Vafaei-Najafabadi N, Marsh KA, Clayton CE, An W, Mori WB, et al. (2014) Hosing instability suppression in self-modulated plasma wakefields. Phys Rev Lett 112: 205001.

36 Rechatin C, Davoine X, Lifschitz A, Ben Ismail A, Lim J, et al. (2009) Observation of beam loading in a laser-plasma accelerator. Phys Rev Lett 103: 194804.

37 Lu W, Tzoufras M, Joshi C, Tsung FS, Mori WB, et al. (2007) Generating multi-GeV electron bunches using single stage laser wakefield acceleration in a 3-D nonlinear regime. Phys Rev ST Accel Beams 10: 061301.

38 Huang K, Li YF, Li DZ, Chen LM, Tao MZ, et al. (2016) Resonantly enhanced betatron hard x-rays from ionization injected electrons in a laser plasma accelerator. Sci Rep 6: 27633.